EUROPEAN ORGANIZATION FOR NUCLEAR RESEARCH

$\bar{p}p$ AND $\bar{p}d$ INTERACTIONS AT THRESHOLD IN GASEOUS H_2 AND D_2 TARGETS

E.G. Auld[1], J.M. Bailey[2], G.A. Beer[3], B. Dreher[4],
H. Drumm[5], K. Erdmann[1], U. Gastaldi[5], H. Kalinowsky[4],
E. Klempt[4], K. Merle[4], K. Neubecker[4], C. Sabev[6],
R.D. Wendling[5], B.L. White[1] and W.R. Wodrich[4],

(Daresbury-Mainz-TRIUMF Collaboration)

ABSTRACT

The $\bar{p}p$ and $\bar{p}d$ interactions at threshold can be studied by comparing the shifts ΔE and the broadening Γ_A of the QED levels of $\bar{p}p$ and $\bar{p}d$ atoms, deduced from the measurement of the energies and intensities of the characteristic X-ray transitions. We report on the first observation of X-rays from $\bar{p}p$ and $\bar{p}d$ atoms formed by stopping antiprotons in H_2 and D_2 gas. The population of the 2P level of antiprotonic hydrogen (protonium) and antiprotonic deuterium was found to be 6 ± 3% at 4 atm and ambient temperature. We present evidence that the 2P levels of antiprotonic hydrogen (deuterium) decay by annihilation at least 10 times (7 times) more frequently than by emission of the K_α X-rays. By selection of specific annihilation channels in coincidence with the observation of L X-rays from $\bar{p}p$ atoms, we establish an upper limit for the yield of K_α X-rays of 0.6% for orthoprotonium and of 0.2% for paraprotonium.

Geneva - 28 May 1978

Paper contributed to the IV European Antiproton Symposium
Barr, France, 26-30 June, 1978

---

1) Department of Physics, University of British Columbia, Vancouver, Canada.

2) Daresbury Laboratory, UK, and Inst. voor Kernphysisch Onderzoek, Amsterdam, The Netherlands.

3) Department of Physics, University of Victoria, Canada.

4) Institut für Kernphysik and Institut für Physik, Universität Mainz, Federal Republic of Germany.

5) CERN, Geneva, Switzerland.

6) Visitor at CERN.

$\bar{p}p$ AND $\bar{p}d$ INTERACTIONS AT THRESHOLD IN GASEOUS H_2 AND D_2 TARGETS

E.G. Auld[1)], J.M. Bailey[2)], G.A. Beer[3)], B. Dreher[4)], H. Drumm[5)], K. Erdmann[1)], U. Gastaldi[5)], H. Kalinowsky[4)], E. Klempt[4)], K. Merle[4)], K. Neubecker[4)], C. Sabev[6)], R.D. Wendling[5)], B.L. White[1)] and W.R. Wodrich[4)]

(Daresbury-Mainz-TRIUMF Collaboration)

ABSTRACT

The $\bar{p}p$ and $\bar{p}d$ interactions at threshold can be studied by comparing the shifts ΔE and the broadening Γ_A of the QED levels of $\bar{p}p$ and $\bar{p}d$ atoms, deduced from the measurement of the energies and intensities of the characteristic X-ray transitions. We report on the first observation of X-rays from $\bar{p}p$ and $\bar{p}d$ atoms formed by stopping antiprotons in H_2 and D_2 gas. The population of the 2P level of antiprotonic hydrogen (protonium) and antiprotonic deuterium was found to be $6 \pm 3\%$ at 4 atm and ambient temperature. We present evidence that the 2P levels of antiprotonic hydrogen (deuterium) decay by annihilation at least 10 times (7 times) more frequently than by emission of the K_α X-rays. By selection of specific annihilation channels in coincidence with the observation of L X-rays from $\bar{p}p$ atoms, we established an upper limit for the yield of K_α X-rays of 0.6% for orthoprotonium and 0.3% for paraprotonium.

---

1) Department of Physics, University of British Columbia, Vancouver, Canada.

2) Daresbury Laboratory, UK, and Inst. voor Kernphysisch Onderzoek, Amsterdam, The Netherlands.

3) Department of Physics, University of Victoria, Canada.

4) Institut für Kernphysik and Institut für Physik, Universität Mainz, Federal Republic of Germany.

5) CERN, Geneva, Switzerland.

6) Visitor at CERN.

The interaction at threshold of antiprotons with protons and deuterons and their annihilation at rest have recently been studied in a number of theoretical [1-12] and experimental [13-28] investigations. Special interest has been focused on the possibility of determining the zero relative momentum scattering lengths for the antinucleon-nucleon interaction from measurements of the energies and widths of low-lying states of the $\bar{p}p$ and $\bar{p}d$ atoms; and on the connection between these states and the structure of possible quasi-nuclear bound states. Further attention is given to the question, From which angular momentum states does annihilation occur when antiprotons are stopped in hydrogen or deuterium? This interest is greatly enhanced by the experimental possibilities offered by the forthcoming cooled antiproton beams [29].

While evidence for the K series of antiprotonic hydrogen has possibly been detected from antiprotons stopped in liquid H_2 [27], we report on the first observation of L X-rays from antiprotonic hydrogen and antiprotonic deuterium atoms, formed by stopping antiprotons in H_2 and D_2 gas. At 4 atm and ambient temperature the absolute yield of the L X-ray radiation emitted in radiative transitions to the $n = 2$ levels of antiprotonic hydrogen or deuterium was found to be $(6 \pm 3)\%$. These X-rays populate mostly the 2P level, and consequently we searched for K_α X-rays by requiring a second X-ray to be present in the K_α X-ray energy range in coincidence with an X-ray in the L energy range. From these coincidence spectra we derive an upper limit of 0.6% (0.9%) for the yield of K_α transitions in antiprotonic hydrogen (deuterium) in a 4 atm gaseous target. Hence the 2P level of antiprotonic hydrogen (deuterium) decays by annihilation at least 10 times (7 times) more frequently than by emission of a K_α X-ray.

A gaseous target was used to form antiprotonic atoms, in order to minimize the probability that collisions with target gas molecules introduce Stark mixing between states of different angular momenta thus leading to annihilation from S or P states at high n levels and preventing the exotic atom from reaching low-lying levels via radiative transitions. The drawback of the low stopping power of gas was compensated by the use, as X-ray detector, of a proportional counter of nearly 4π angular acceptance and a threshold for X-ray detection of about 1 keV. The difficulty of assigning a signature to antiproton stops in gas was overcome by a 50 μ thin entrance scintillation counter inside the gas, which identified antiprotons at the very end of their range.

The experiment was performed at the m_{14} low-momentum antiproton beam of the CERN Proton Synchrotron (PS) [30] (typically 2000 $\bar{p}$/burst at 900 MeV/c; $\pi^-/\bar{p}$ contamination $\sim$ 10). The beam was moderated in energy by a Cu degrader before entering the target gas. The thickness of the moderator was adjusted to place the counter gas at the peak of the $\bar{p}$ range curve (Fig. 1c). Antiprotons entering the experimental target [31] (Figs. 1a, 1b) were defined by a counter telescope $(B_1B_2)_{TOF}\check{C}T_1T_2\bar{T}_3$ and called stop CANDIDATES.

A 4π system of plastic scintillators installed inside the pressure vessel gave a fast definition of a $\bar{p}$-STOP signal; this was checked periodically against its pressure dependence (Fig. 1d). Charged annihilation prongs were identified by the proportional counter cells, the surrounding E scintillators, and scintillation counters installed outside the pressure tank.

The X-ray detector consisted of an array of 36 independent gas proportional counter cells X_i surrounding the target gas volume [32], and separated from it by a 12 μm thick mylar foil. The H_2 target and the X-ray counter operated at the same pressure of 4 atm. Target gas and proportional counter gas (argon + 5% propane) were continuously flushed, to avoid mutual contamination. The calculated average efficiency for detecting an X-ray produced at a typical point in the target is shown by the smooth line in Figs. 2a and 3a. The efficiency given in these figures must be multiplied by a factor, depending on the $\bar{p}p$ annihilation mode, which takes into account the average number of cells of the X-ray detector that were not usable for detecting X-rays because of charged annihilation prongs traversing them. If a charged particle had traversed the proportional counter cell X_i, five contiguous cells X_j $(i-2 \leq j \leq i+2)$ were excluded from the analysis to eliminate fluorescence produced in the counter gas or δ-rays propagating directly between adjacent cells of the counter.

The in-beam gain and resolution of each cell were continuously calibrated during the measurements, using the 5.5 keV line from a weak ^{54}Mn source installed on the centre of the scintillation counter T_4 (dotted spectrum in Fig. 2a) and the 3.0 keV fluorescence line from the argon counter gas (histogram in Figs. 2a and 3a). The trigger for the calibration spectra was provided by signals in scintillator T_4 from 835 keV γ-rays that are emitted in all ^{54}Mn decays, and by the coincidence $(B_1B_2)_{TOF}\overset{\bar{\gamma}}{C}T_1T_2\bar{T}_3\bar{T}_4E$ (outward-scattered heavily ionizing particles that have a high chance of exciting argon fluorescence).

Spectra from all 36 proportional counters were added following a gain-normalizing correction for each individual counter determined from the calibration spectra. For the added spectra the in-beam (FWHM) resolution was about 25% at 5.5 keV and 35% at 3 keV.

Each signal in a given proportional counter produced three separate outputs, which were recorded when triggered by a CANDIDATE pulse, and provided for every signal i) the total charge E_x, ii) the rise-time t_r, and iii) the delay t_d versus the trigger time. Each CANDIDATE trigger generated an event record containing E_x, t_r, and t_d for each of the 36 proportional cells which had responded, the pattern of the coincidences defining the STOP trigger and the pattern of E counters which fired on minimum ionizing particles. X-ray spectra were obtained from the event records by accepting only those proportional counter pulses with rise-times lying in the X-ray rise-time window determined in-beam from the X-ray calibration spectra. This allows rejection of most of the pulses produced by charged particles scattered through the proportional counter, since these pulses are due to the amplification of all the clusters of primary electrons produced along ionizing tracks and are then longer in rise-time than X-ray pulses which are originated by one isolated cluster. Data for all triggers were taken at the same time; the different triggers were indicated, event by event, by a CAMAC flag. Identical rise-time and drift-time cuts have been applied to all of the data.

The data on antiprotonic hydrogen and an antiprotonic deuterium presented here were collected in a period of totally 640 hours, corresponding to 150,000 stops in H_2 gas and 50,000 stops in D_2 gas. The resulting spectra are shown in Figs. 2 and 3 without applying any kind of background subtraction. The average energy resolution was slightly worse during the D_2 runs. For a direct comparison of $\bar{p}p$ and $\bar{p}d$ data we have therefore plotted in Fig. 3 the $\bar{p}p$ data which were taken immediately before and after the $\bar{p}d$ runs (dotted lines). These data were collected with the same number of antiproton stops and the same in-beam resolution.

The spectra in Figs. 2b and 3b were generated by requiring a STOP trigger and, in addition, that only one X counter, X_i, among the 36 should have recorded a signal, and that this signal should lie within the X-ray rise-time window. This condition meant that no charged particle had traversed the proportional counter gas, so that in particular no argon fluorescence background should be present in this spectrum. Spectra 2c and 3c were generated requiring a STOP trigger only, and therefore can contain background X-rays generated in materials other than the target gas by charged particles from $\bar{p}$ annihilations.

The low-energy peaks in the spectra of Figs. 2b and 3b are interpreted as being due to the L X-rays from $\bar{p}p$ and $\bar{p}d$ atoms for the following reasons: evidently, the energies are consistent with the QED L X-ray energies indicated in the figures, and the peaks in Figs. 3b and 3c compared to the peaks in Figs. 2b and 2c are shifted towards the higher energy region, as was expected from the increase by a factor of 4/3 of the reduced mass of the radiating system. The spectrum obtained when He was substituted for H_2 or D_2 shows completely different topology, as the $\bar{p}$He X-ray lines dominate the argon fluorescence signal and are distant in energy from the $\bar{p}p$ and $\bar{p}d$ lines [33]. Therefore we conclude that the low-energy X-ray peaks originate from the *target gas* and are not, apart from the argon fluorescence line in Figs. 2c and 3c, produced in the surrounding materials of the target. Only the K series of π^-p and π^-d could simulate the observed energy shift when changing the target gas from H_2 to D_2, but the fraction of pions associated with the STOP trigger, stopping in the target gas and emitting a K line, was estimated to be negligible. In any case, the K series of π^-p and π^-d could contribute only to the spectra of Figs. 2b and 2c, as no charged particles are emitted in these annihilations.

Several additional checks were carried out, including the use of different proportional counter gases, which supported this interpretation of the data [34]. Therefore we conclude that X-rays from antiprotonic hydrogen and deuterium atoms have been detected and that these new exotic atoms have been observed for the first time.

The determination of the absolute yield of the L X-ray radiation from the spectra of Figs. 2c and 3c and from the pressure curve of Fig. 1d requires the subtraction of the contribution of argon fluorescence and, because of the steep energy dependence of the detection efficiency, the knowledge of the relative contributions of the different lines of the L series. Therefore the peaks of Figs. 2b and 3b were fitted, after subtraction of a smooth background, with three lines (i.e. L_α, L_β and one line representing the convolution of the lines L_γ ... L_∞) with energies fixed at the QED values and instrumental widths obtained by scaling the widths of the 3 keV and 5.5. keV calibration lines; this was done in order to find their relative intensities. The absolute intensities were then derived by fitting the spectra of Figs. 2c and 3c with these three lines of fixed relative intensities plus a line of free intensity at 3 keV to establish the contribution of the argon fluorescence line. Taking into account the detection efficiency, the number of cells discarded for poor resolution, and the percentage of cells inhibited by the charged annihilation products, an absolute yield of L X-ray transitions per stopped antiproton of $(6.1 \pm 3.0)\%$ from antiprotonic hydrogen and $(5.5 \pm 3.0)\%$ from antiprotonic deuterium is determined.

On the other hand, there is no obvious line in the 6-12 keV energy range where K X-rays may be expected. Therefore we searched for K_α X-rays in coincidence with L X-rays to reduce the over-all background.

Figure 2d (3d) shows a spectrum containing those X-rays of Fig. 2c (3c) which are accompanied by another X-ray, X_1, present in the same STOP trigger and detected in a separate cell with energy in the bin window X_1 indicated in the drawing. The X_1 X-ray has an energy compatible with all L transitions. From the total number of L X-rays present in the spectrum 2c (3c) and falling in the X_1 energy region, and from the maximum number of counts weighted by the efficiency in any 2 keV wide energy region (to account for the instrumental resolution and a strong widening of the K_α line) in the spectrum 2d (3d), we conclude that an L transition is followed in less than 10% (15%) of the cases by a K_α transition. Hence the total yield of K_α transitions is less than 0.6% (0.9%) and the dominant decay mode of the 2P level is annihilation since the probability of Stark mixing at the $n = 2$ level is negligible in gas.

Finally, Fig. 2e shows the coincidence spectrum where one X-ray falls into the X_1 energy region, a second X-ray is detected in a separate cell, and where, in addition, no charged particle has traversed the proportional counter gas, nor has been detected in one of the scintillation counters surrounding the target. K X-rays followed by annihilation of the $\bar{p}p$ atom into neutral pions identify the final state as a spin singlet $1\,^1S_0$ state, since the decay of $\bar{p}p \to n\pi^0$ is forbidden from even-L spin triplet states and other neutral decay modes are rare. Therefore the spectrum of Fig. 2e allows us to derive independently an upper limit of 0.2% for the yield of K_α X-ray emission from the 2P state of the spin singlet system of protonium (paraprotonium). This upper limit is obtained considering that the fraction of annihilations from the $^1S_0$ states into neutrals only should exceed 10%, under the assumption of a statistical population of singlet and triplet S states at high n, and taking into account that

i) the branching ratio for annihilations into neutrals only, when antiprotons are stopped in liquid H_2, is 3.3%;

ii) annihilation from S states is expected to dominate P wave annihilation in liquid H_2; and

iii) the L X-rays in the "0-prong" spectrum represent 5% of the total L X-ray yield in H_2 gas at 4 atm.

The radiative width of the 2P level of $\bar{p}p$ is 0.37 meV and of $\bar{p}d$ 0.5 meV. The upper limits for the decay branching ratios for K_α X-ray emission from the 2P states therefore imply a lower limit of 4 meV for the strong interaction widths of the 2P levels of antiprotonic hydrogen and antiprotonic deuterium.

REFERENCES

[1] T.B. Day, G.A. Snow and J. Sucher, Phys. Rev. 118 (1960) 864.

[2] S. Caser and R. Omnès, Phys. Letters 39B (1972) 369.

[3] O.D. Dalkarov and V.M. Samoilov, JETP Letters 16 (1972) 249.

[4] O.D. Dalkarov and B.O. Kerbikov, JETP Letters 21 (1975) 134.

[5] V.E. Markushin, Preprint ITEP-164, Moscow (1976).

[6] W.B. Kaufman and H. Pilkuhn, Phys. Letters 62B (1976) 165.

[7] T.E.O. Ericson, Low-energy $\bar{N}N$ interactions, Proc. 3rd European Symposium on Antinucleon-Nucleon Interactions, Stockholm, 1976 (eds. G. Ekspong and S. Nilsson) (Pergamon Press, Oxford, 1977), p. 3.

[8] T.E.O. Ericson and L. Hambro, Ann. Phys. 107 (1977) 44.

[9] O.D. Dalkarov, Preprint ITEP-135, Moscow (1977).

[10] B. Kerbikov, Preprint CERN-TH 2394 (1977).

[11] H. Pilkuhn and S. Wycech, Preprint TKP 77-17, Karksruhe (1977).

[12] I.S. Shapiro, Phys. Reports 35C (1978) 131.

[13] R. Bizzarri, Threshold and low-energy phenomena. Invited talk given at this conference.

[14] For a review of previous activity on protonium, see R.E. Welsh, Exotic atoms (K^-, $\bar{p}$, Σ^-), Proc. 7th Internat. Conf. on High-Energy Physics and Nuclear Structure, Zurich, 1977 (ed. M.P. Locher) (Birkhäuser Verlag, Basel and Stuttgart, 1977), p. 95.

[15] R. Armenteros, D.N. Edwards, T. Jacobsen, L. Montanet, J. Vandermeulen, Ch. d'Andlau, A. Astier, P. Baillou, J. Cohen-Ganouna, C. Defoix, J. Siaud and P. Rivet, Phys. Letters 17 (1965) 344.

[16] C. Baltay, N. Barash, P. Franzini, N. Gelfand, L. Kirsch, G. Lütjens, D. Miller, J.C. Severiens, J. Steinberger, T.H. Tan, D. Tycko, D. Zanello, R. Goldberg and R.J. Plano, Phys. Rev. Letters 15 (1965) 532.

[17] S. Devons, T. Kozlowski, P. Nemethy, S. Shapiro, N. Horwitz, T. Kalogeropoulos, J. Skelly, R. Smith and H. Uto, Phys. Rev. Letters 27 (1971) 1614.

[18] L. Gray, P. Hagerty and T. Kalogeropoulos, Phys. Rev. Letters 26 (1971) 1491.

[19] L. Gray, Theo. Papadopoulou, E. Simopoulou, A. Vayaki, T. Kalogeropoulos and J. Roy, Phys. Rev. Letters 30 (1973) 1091.

[20] R. Bizzarri, G. Ciapetti, U. Dore, M. Gaspero, I. Laakso, F. Marzano and G.C. Moneti, Nuclear Phys. B 69 (1974) 298.

[21] R. Bizzarri, G. Ciapetti, U. Dore, M. Gaspero, I. Laakso, F. Marzano and G.C. Moneti, Nuclear Phys. B 69 (1974) 307.

[22] T.E. Kalogeropoulos and G.S. Tzanakos, Phys. Rev. Letters 34 (1975) 1047.

[23] C.R. Sun, S. Dhar, M. Dickinson and B. Krinsky, Phys. Rev. D 14 (1976) 1188.

[24] G. Bassompierre, G. Binder, P. Dalpiaz, P.F. Dalpiaz, G. Gissinger, S. Jacquey, C. Peroni, M.A. Schneegans and L. Tecchio, Determination of the proton electromagnetic form factors at and near threshold of the time-like region. Contributed paper to this conference. See also Phys. Letters 68B (1977) 477.

[25] G. Bassompierre, G. Binder, P. Dalpiaz, P.F. Dalpiaz, G. Gissinger, S. Jacquey, C. Peroni, M.A. Schneegans and L. Tecchio, Measurement of the $\pi^0\pi^0$ production in $\bar{p}p$ annihilation at rest. Contributed paper to this conference.

[26] L. Tauscher, G. Backenstoss, P. Blüm, K. Fransson, R. Guigas, N. Hassler, M. Izycki, H. Koch, A. Nilsson, P. Pavlopoulos, H. Poth, M. Suffert and K. Zioutas, Measurement of the γ-ray spectrum produced by the $\bar{p}p$ system at rest. Contributed paper to this conference. See also Phys. Letters 72B (1978) 415.

[27] M. Izycki, G. Backenstoss, P. Blüm, K. Fransson, R. Guigas, N. Hassler, H. Koch, A. Nilsson, P. Pavlopoulos, H. Poth, M. Suffert, L. Tauscher and K. Zioutas, Results on the measurements of K-series X-rays from antiprotonic hydrogen. Contributed paper to this conference.

[28] E. Borie, X-ray yields from protonium. Contributed paper to this conference.

[29] U. Gastaldi, $\bar{p}p$ experiments at low energy using cooled antiprotons. Invited talk given at this conference.

[30] G. Bassompierre, G. Binder, P. Dalpiaz, P.F. Dalpiaz, M. Ferro-Luzzi, G. Gissinger, S. Jacquey, C. Peroni, F.M. Schmitt, M.A. Schneegans and L. Tecchio, Nuclear Instrum. Methods 40 (1977) 251.

[31] E.G. Auld, H. Averdung, J. Bailey, G.A. Beer, B. Dreher, K.L. Erdman, U. Gastaldi, E. Klempt, K. Merle, K. Neubecker, Ch. Sabev, H. Schwenk, R.D. Wendling, B.L. White and R. Wodrich, An apparatus with 4π angular acceptance and high efficiency for the detection of X-rays in the 1-15 keV energy region from exotic atoms formed in H_2, D_2, and He gas in the pressure range 0.5-16 abs. atm. To be submitted to Nuclear Instrum. Methods.

[32] U. Gastaldi, R.D. Wendling, E.G. Auld, H. Averdung, J. Bailey, G.A. Beer, B. Dreher, K.L. Erdman, E. Klempt, K. Merle, K. Neubecker, Ch. Sabev, H. Schwenk, B.L. White and R. Wodrich, A cylindrical multiwire high-pressure gas proportional chamber surrounding a gaseous H_2 target with mylar separation foil 6 μm thick, presented at the Wire Chamber Conference, Vienna, 1978.

[33] E.G. Auld, J. Bailey, G.A. Beer, B. Dreher, U. Gastaldi, H. Kalinowski, E. Klempt, K. Merle, K. Neubecker, R.D. Wendling, B.L. White and R. Wodrich, X-ray transitions from antiprotonic helium gas. To be submitted to Phys. Letters.
See also U. Gastaldi, The X-ray drift chamber (XDC), to be published in Nuclear Instrum. Methods (1978).

[34] E.G. Auld, H. Averdung, J.M. Bailey, G.A. Beer, B. Dreher, H. Drumm, K. Erdman, U. Gastaldi, E. Klempt, K. Merle, K. Neubecker, C. Sabev, H. Schwenk, V.H. Walther, R.D. Wendling, B.L. White and W.R. Wodrich, First observation of X-rays from antiprotonic hydrogen, to be published in Phys. Letters B.

Figure captions

Fig. 1 : Side view (1a) and front view (1b) of the apparatus: Incident $\bar{p} = (B_1B_2)_{TOF}\overline{\check{C}}$; $\bar{p}$ stop CANDIDATE trigger = $= (B_1B_2)_{TOF}\overline{\check{C}}T_1T_2\bar{T}_3$; $\bar{p}$ STOP trigger $= (B_1B_2)_{TOF}\overline{\check{C}}T_1T_2\bar{T}_3\bar{T}_4\overline{\Sigma E}_H$; ΣE_H is the output of an OR unit fed by E_H discriminators with high threshold so as not to veto on annihilation prongs. Range curve (1c), with C the external degrader ($\rho = 1.84$ g/cm^2). Pressure curve (1d) taken with 4.5 cm thick C degrader.

Fig. 2 : X-ray detection efficiency of the array of 36 proportional cells (2a, smooth line). ^{54}Mn in beam calibration spectrum; 835 keV γ trigger; peak at 5.5 keV (2a, dotted curve). X-ray spectrum with outward-scattered CANDIDATE trigger = $= (B_1B_2)_{TOF}\overline{\check{C}}T_1T_2\bar{T}_3\bar{T}_4\Sigma E$; the peak at 3 keV is the Ar fluorescence line (2a, histogram). X-ray spectrum with "STOP and 0-prong annihilation" trigger; the peak in the 2-3 keV region is from $\bar{p}p$ L transitions (2b). X-ray spectrum with STOP trigger; the asymmetric peak in the 2-3 keV region is from $\bar{p}p$ L lines and Ar fluorescence line (2c). X-ray spectrum with "STOP and one coincident X-ray in the X_1 energy region" trigger (2d). X-ray spectrum with "STOP, 0-prong annihilation, and one coincident X-ray in the X_1 energy region" trigger (2e).

Fig. 3 : X-ray detection efficiency of the array of 36 proportional cells (3a, smooth line). X-ray spectrum with outward-scattered CANDIDATE trigger $= (B_1B_2)_{TOF}\overline{\check{C}}T_1T_2\bar{T}_3\bar{T}_4\Sigma E$; the peak at 3 keV is the Ar fluorescence line (3a, histogram). X-ray spectrum with "STOP and 0-prong annihilation" trigger; the peak in the 3-5 keV region is from $\bar{p}d$ L transitions (3b). X-ray spectrum with STOP trigger; the asymmetric peak in the 3-5 keV region is from $\bar{p}d$ L lines and Ar fluorescence line (3c). X-ray spectrum with "STOP and one coincident X-ray in the X_1 energy region" trigger (3d).

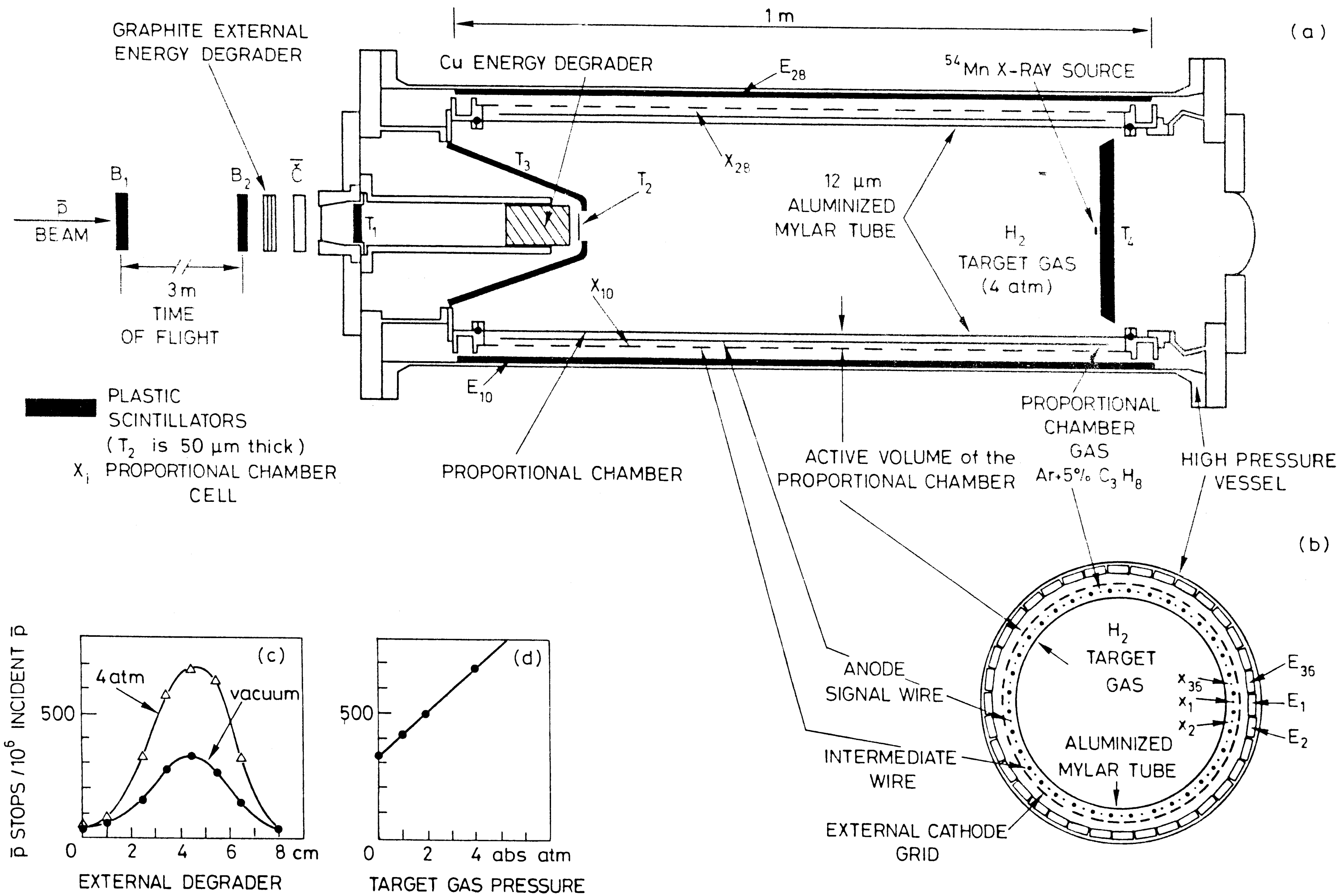
GRAPHITE EXTERNAL ENERGY DEGRADER
1 m
(a)
Cu ENERGY DEGRADER
E28
54Mn X-RAY SOURCE
B1
B2
C̄
p̄ BEAM
T1
T3
T2
X28
12 µm ALUMINIZED MYLAR TUBE
H2 TARGET GAS (4 atm)
T4
3 m TIME OF FLIGHT
X10
E10
PLASTIC SCINTILLATORS
(T2 is 50 µm thick)
Xi PROPORTIONAL CHAMBER CELL
PROPORTIONAL CHAMBER
ACTIVE VOLUME of the PROPORTIONAL CHAMBER
PROPORTIONAL CHAMBER GAS Ar+5% C3 H8
HIGH PRESSURE VESSEL
(b)
H2 TARGET GAS
ALUMINIZED MYLAR TUBE
ANODE SIGNAL WIRE
INTERMEDIATE WIRE
EXTERNAL CATHODE GRID
E36
E1
E2
x35
x1
x2
p̄ STOPS / 10^6 INCIDENT p̄
(c)
4 atm
vacuum
500
0
2
4
6
8 cm
EXTERNAL DEGRADER
(d)
4 abs atm
TARGET GAS PRESSURE

Fig. 1

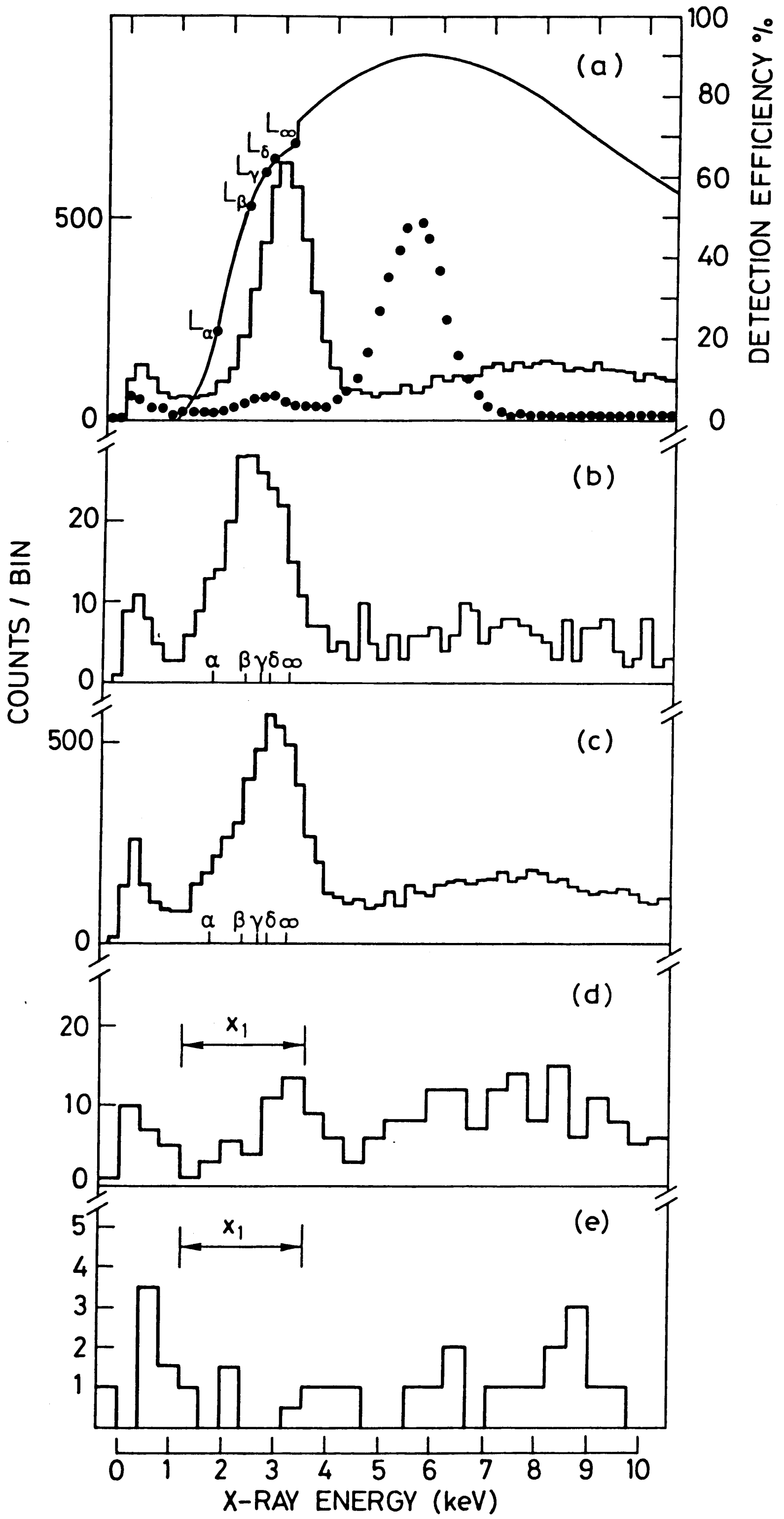

(a)
(b)
(c)
(d)
(e)
DETECTION EFFICIENCY %
COUNTS / BIN
X-RAY ENERGY (keV)
L_α
L_β
L_γ
L_δ
L_∞
α β γ δ ∞
x_1
0 1 2 3 4 5 6 7 8 9 10
0 20 40 60 80 100
0 500
0 10 20
0 1 2 3 4 5

Fig. 2

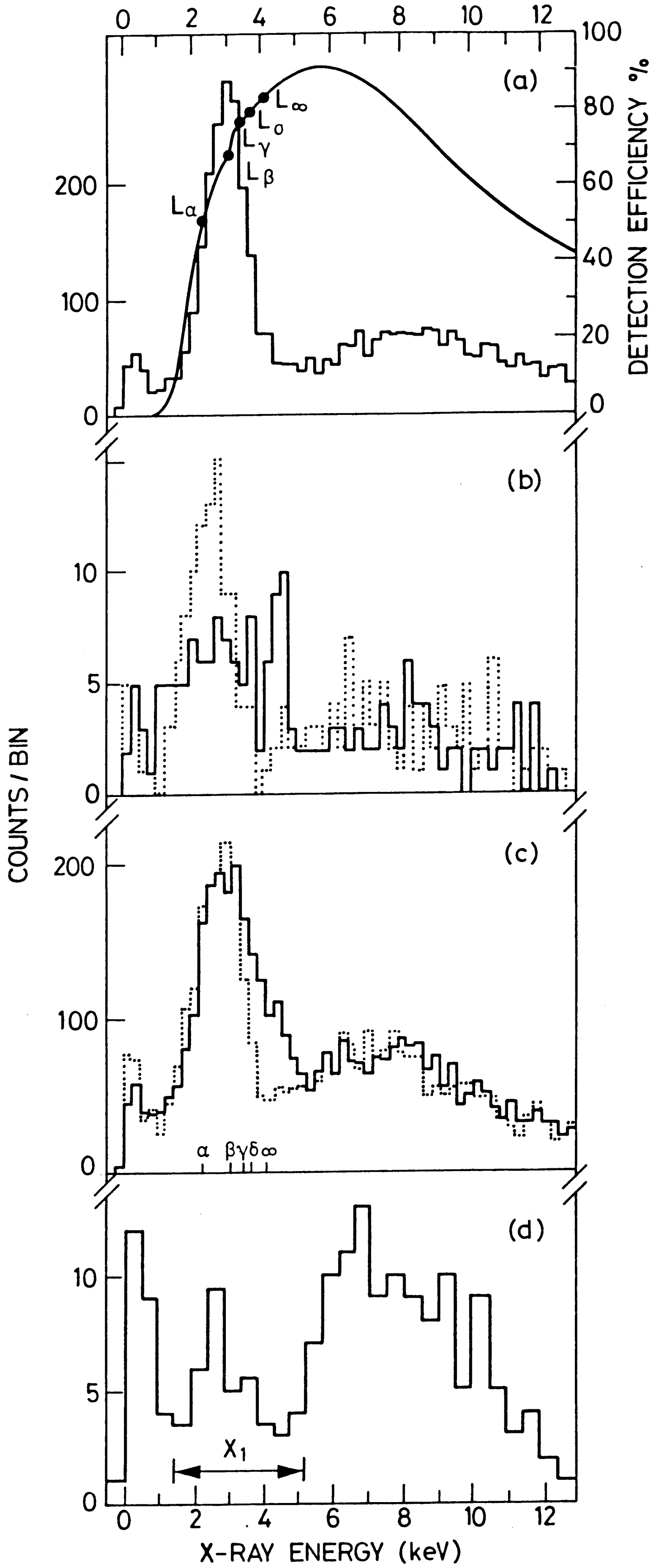

(a)
(b)
(c)
(d)
COUNTS / BIN
DETECTION EFFICIENCY %
X-RAY ENERGY (keV)
Lα
Lβ
Lγ
Lδ
L∞
α βγδ∞
X1

Fig. 3